

Уравнение состояния нейтронной материи в модели Составного кваркового мешка

М.И. Криворученко
ИТЭФ, Москва

М.И.К., Phys. Rev. C, 82, 018201 (2010)
М.И.К., Phys. Rev. C, 84, 015206 (2011)
М.И.К., Письма в ЭЧАЯ (2017), в печати.

- Аналитичность и унитарность в модели СКМ
- КДД полюса, ассоциированные с примитивами Джаффе-Лоу
- Конверсия «примитив-резонанс» и узкие дибарионы
- Сверхпроводимость, E_0 нейтронной материи

Семинар БЛТФ, ОИЯИ
Дубна, 14 июня 2017

INTRODUCTION

$$A(s,t) = \sum_R \text{[t-channel diagram]} = \sum_P \text{[s-channel diagram]}$$

NN INTERACTION MODELS:

t-channel vs. s-channel



Exchange of $\bar{q}q$ -mesons
Yukawa mechanism

95% of the market



Lee-Dyson model,
QCB model:

Exchange of bq -primitives

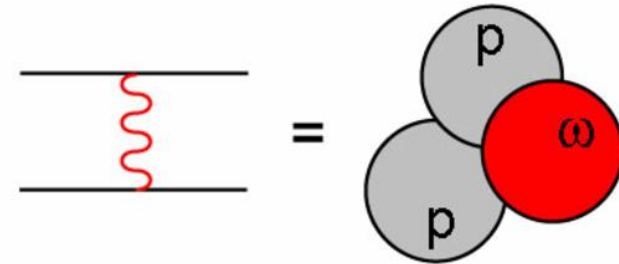
$$A(s,t) = \sum_{R,P} \text{[t-channel diagram]} \neq \sum_{R,P} \text{[s-channel diagram]}$$



THESE TWO MECHANISMS MAY APPEAR **MUTUALLY EXCLUSIVE** OR **DUAL** TO EACH OTHER.

Motivation for an s -channel NN interaction model

NO FREE SPACE in nuclei
for t -channel meson exchange:



The sphere of radius r is empty, the nearest neighbor is located in $dV = 4\pi r^2 dr$

HOLZMARK DISTRIBUTION:

$$dw = \exp(-\rho V) \rho dV$$

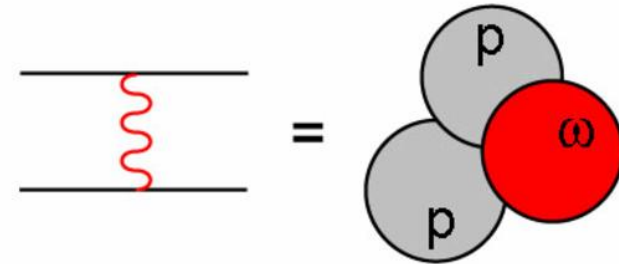
Poisson law:

$$p_k = \frac{\bar{n}^k}{k!} e^{-\bar{n}},$$

$$\bar{n} = \rho V.$$

Motivation for an s -channel NN interaction model

NO FREE SPACE in nuclei
for t -channel meson exchange:



The sphere of radius r is empty, the nearest neighbor is located in $dV = 4\pi r^2 dr$

HOLZMARK DISTRIBUTION:

$$dw = \exp(-\rho V) \rho dV$$

Poisson law:

$$p_k = \frac{\bar{n}^k}{k!} e^{-\bar{n}},$$

$$\bar{n} = \rho V.$$

$$E[r] \pm (\text{Var}[r])^{1/2} = \begin{cases} 1.02 \pm 0.37 \text{ fm,} & \text{without correlations,} \\ 1.18 \pm 0.31 \text{ fm,} & \text{with correlations.} \end{cases}$$

$$\left\langle r^2 \right\rangle_p^{1/2} = 0.8750 \pm 0.0068 \text{ fm,} \quad \left\langle r^2 \right\rangle_\pi^{1/2} = 0.659 \pm 0.025 \text{ fm}$$

Motivation for an s -channel NN interaction model

Neutron stars with mass $2M_{\odot}$ are observed

P. B. Demorest et al., Nature 467, 1081 (2010).

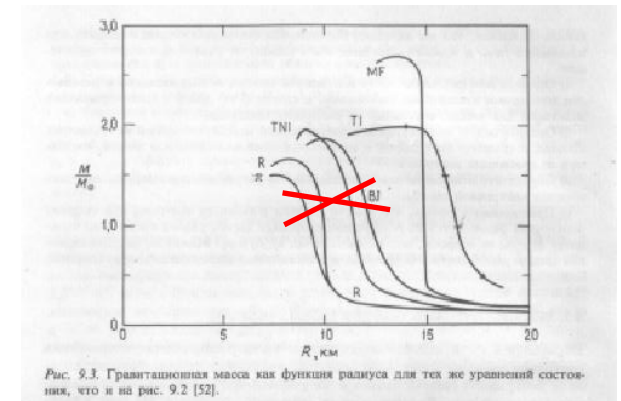
J. Antoniadis et al., Science 340, 448 (2013).

• **Soft EoS of t -channel OBE models are excluded,**

in particular

- pion/kaon condensate EoS
- Reid soft core model
for NN interaction potential
- All earlier hyperon EoS

S. L. Shapiro and S. A. Teukolsky,
**Black Holes, White Dwarfs, and
Neutron Stars, (Cornell U., N. Y., 1983)**



HYPERONS EFFECT ON MASSES OF NEUTRON STARS

At high density the production of hyperons becomes energetically favorable:

V. A. Ambartsumyan and G. S. Saakyan, *Astron. Zh.* 37, 193 (1960).

In the EoS based on the Reid soft core model, the inclusion of hyperons **drops the maximum mass of neutron stars** from $1.6 M_{\odot}$ down to $1.4 M_{\odot}$.

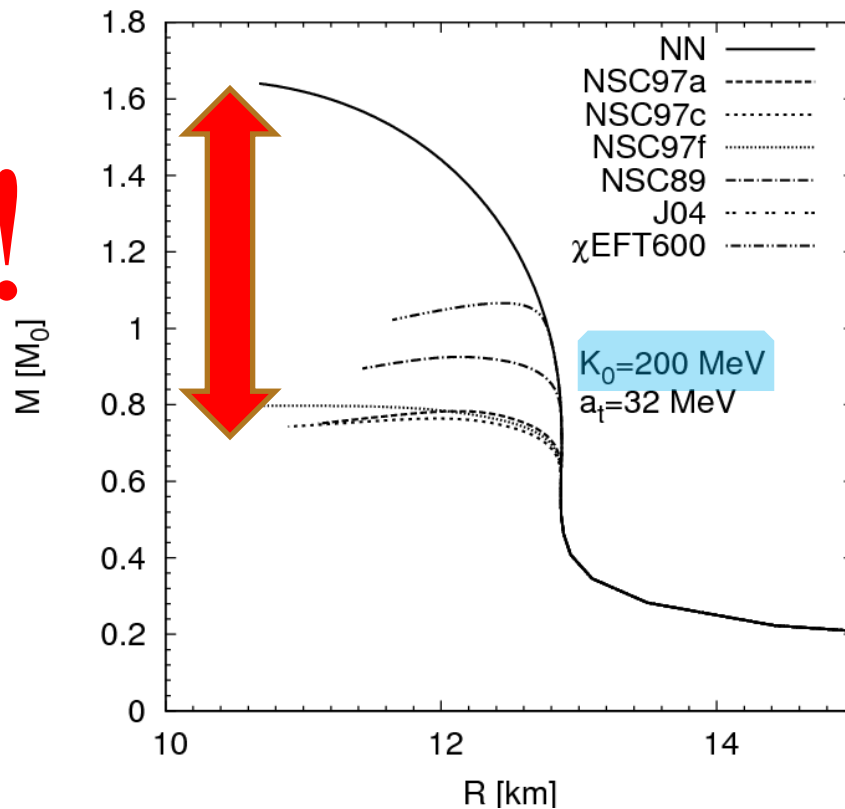
V. R. Pandharipande, R. A. Smith, *Nucl. Phys. A*237, 507 (1975).

HYPERONS EFFECT ON MASSES OF NEUTRON STARS

DBHF model with hyperons from:

H. Djapo, B.-J. Schaefer and J. Wambach, Phys. Rev. C81, 035803 (2010)

?!

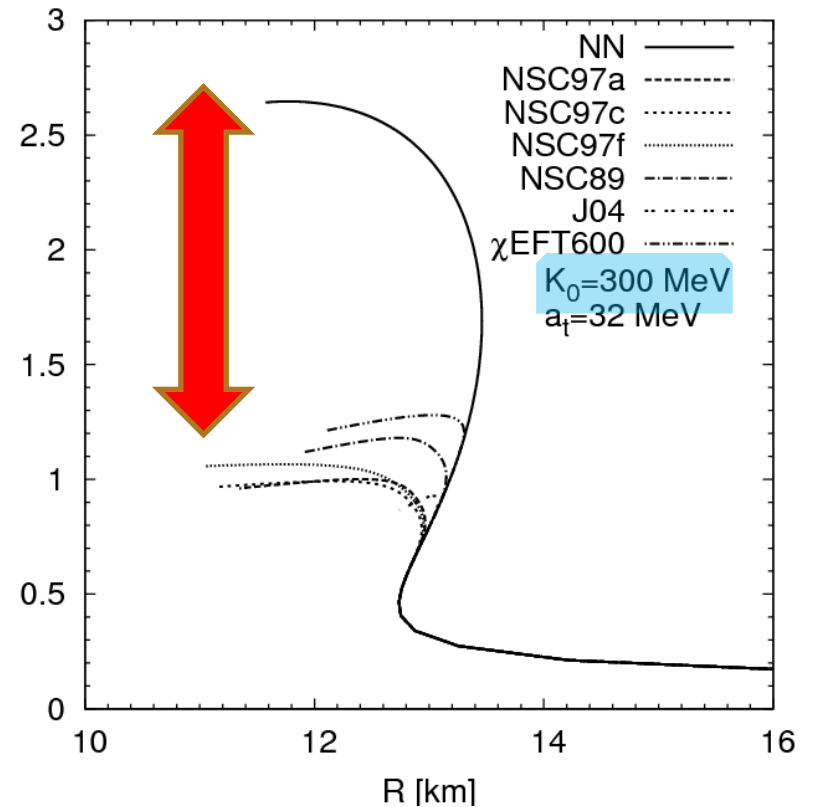
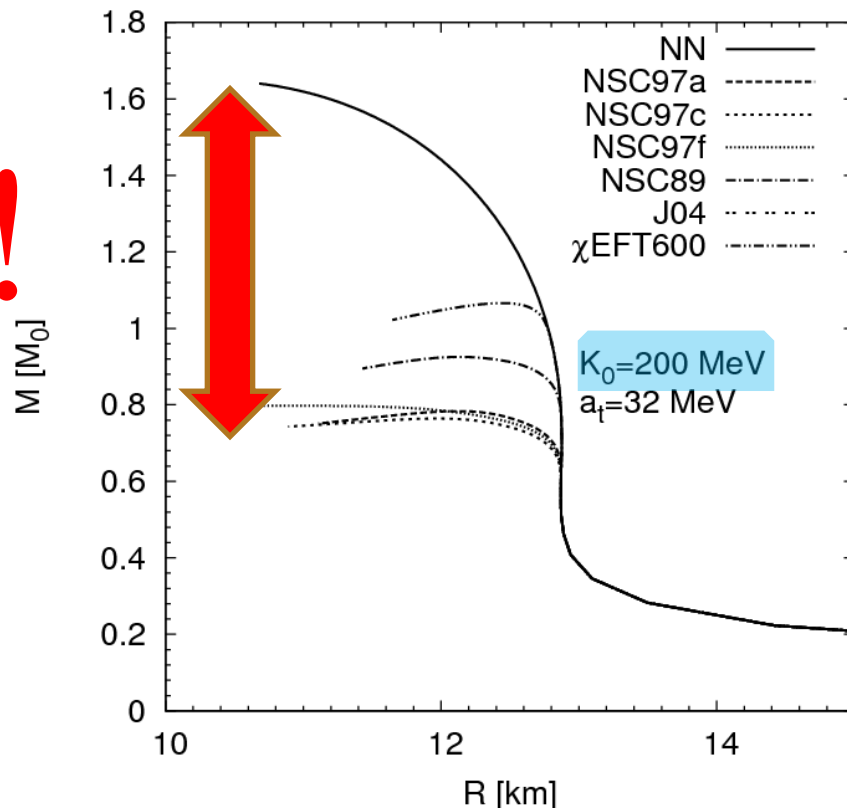


HYPERONS EFFECT ON MASSES OF NEUTRON STARS

DBHF model with hyperons from:

H. Djapo, B.-J. Schaefer and J. Wambach, Phys. Rev. C81, 035803 (2010)

?!



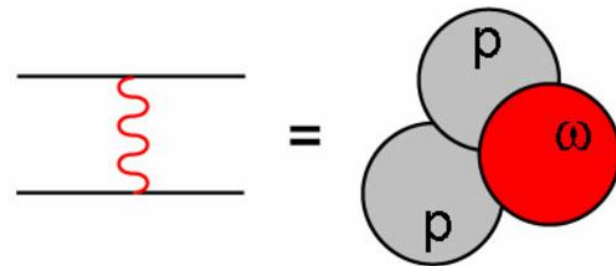
POSSIBLE REASONS OF LOW MASSES OF THE HYPERON STARS:

- 1. Inadequacy of OBE models of nuclear matter at high densities**
- 2. Poor knowledge of the interaction forces between hyperons**
- 3. Missing contribution of new exotic particles - WILBs**

POSSIBLE REASONS OF LOW MASSES OF THE HYPERON STARS:

1. Inadequacy of OBE models of nuclear matter at high densities
2. Poor knowledge of the interaction forces between hyperons
3. Missing contribution of new exotic particles - WILBs

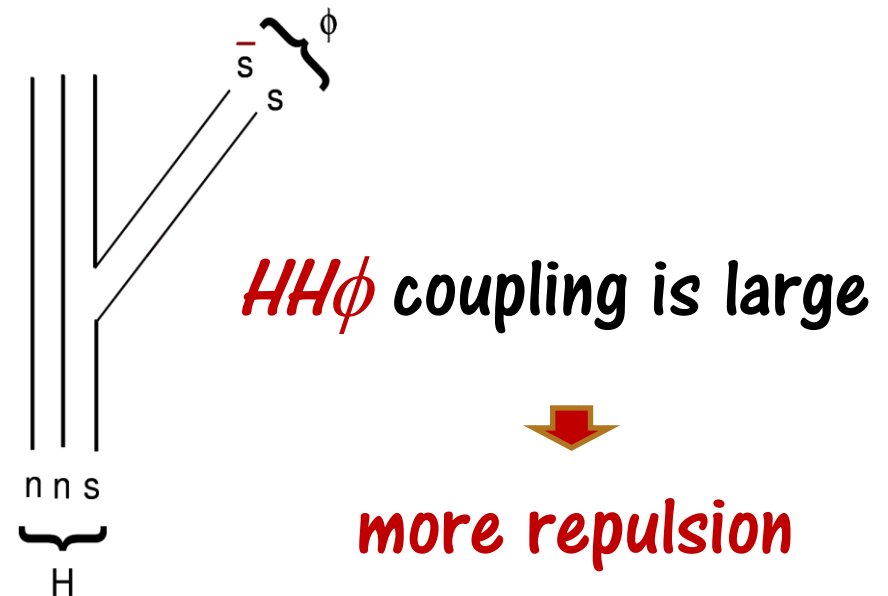
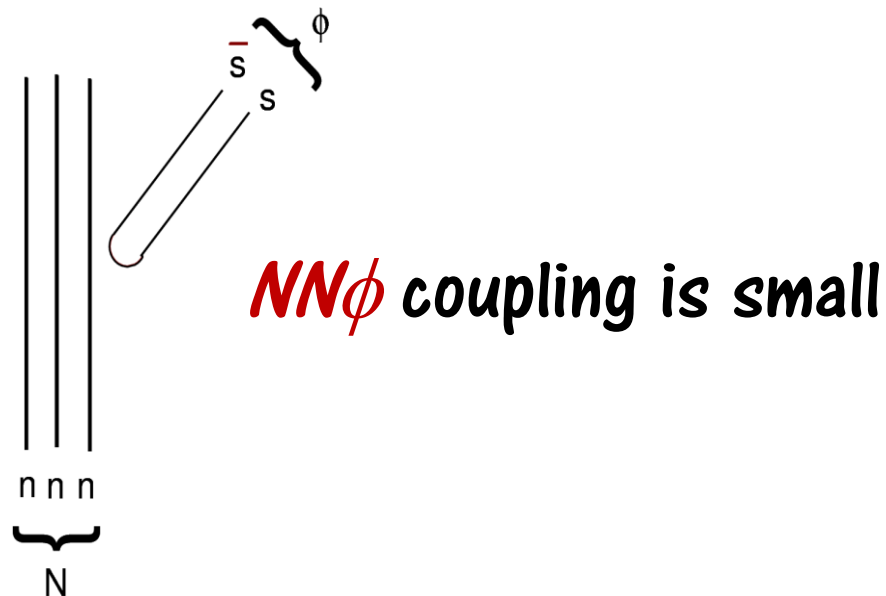
**NO FREE SPACE in nuclei
for t -channel meson exchange:**



POSSIBLE REASONS OF LOW MASSES OF THE HYPERON STARS:

1. Inadequacy of OBE models of nuclear matter at high densities
2. **Poor knowledge of the interaction forces between hyperons**
3. Missing contribution of new exotic particles - WILBs

$\phi(1020)$ -meson subjected to **the OZI rule**
is appropriate to make a stiff EoS



POSSIBLE REASONS OF LOW MASSES OF THE HYPERON STARS:

1. Inadequacy of OBE models of nuclear matter at high densities
2. **Poor knowledge of the interaction forces between hyperons**
3. Missing contribution of new exotic particles - WILBs

A quantitative analysis of the $\phi(1020)$ -meson role

R. Lastowiecki, D. Blaschke, H. Grigorian and S. Typel, Acta Phys. Polon. Supp. 5, 535 (2012)

S. Weissenborn, D. Chatterjee, and J. Schaffner-Bielich, Phys. Rev. C 85, 065802 (2012)

confirmed our conjecture about its influence on EoS

M.I.K., F. Simkovic, Amand Faessler, Phys. Rev. D 79, 125023 (2009).

POSSIBLE REASONS OF LOW MASSES OF THE HYPERON STARS:

1. Inadequacy of OBE models of nuclear matter at high densities
2. Poor knowledge of the interaction forces between hyperons
3. **Missing contribution of new exotic particles - WILBs**

The effect of a vector boson on the energy density:

$$E_I = \frac{1}{2} \int dx_1 dx_2 \rho \frac{g^2}{4\pi r} e^{-\mu r} \rho = V \frac{g^2 \rho^2}{2\mu^2}.$$

Vector WILBs cf. ω -mesons

$$\frac{g^2}{\mu^2} \approx \frac{g_\omega^2}{\mu_\omega^2} \approx 200 \text{ GeV}^{-2}.$$

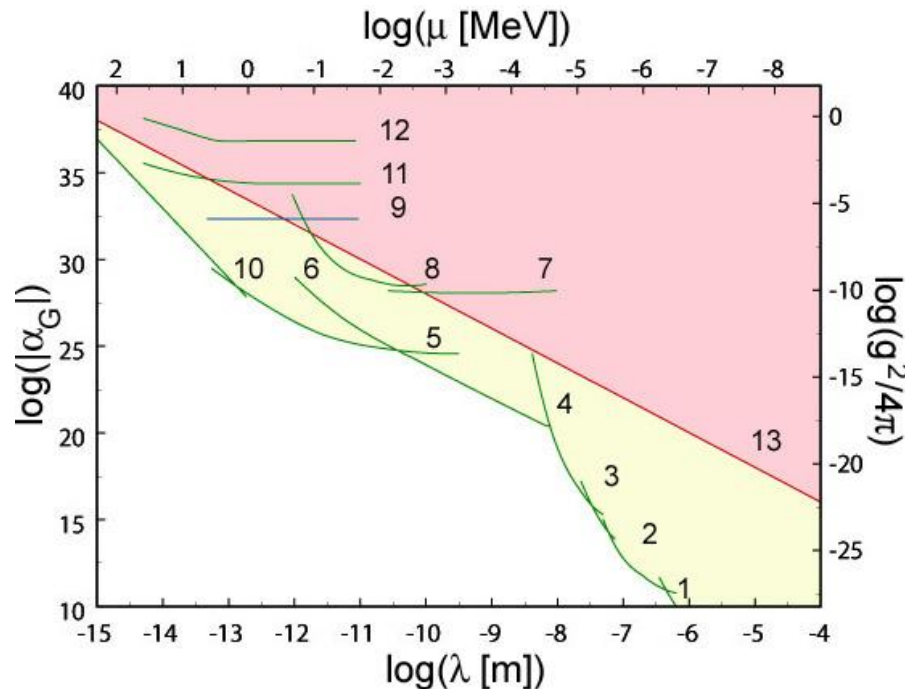
Scalar WILBs cf. σ -mesons

$$\frac{g^2}{\mu^2} \approx \frac{g_\sigma^2}{\mu_\sigma^2} \approx 300 \text{ GeV}^{-2}.$$

POSSIBLE REASONS OF LOW MASSES OF THE HYPERON STARS:

1. Inadequacy of OBE models of nuclear matter at high densities
2. Poor knowledge of the interaction forces between hyperons
3. **Missing contribution of new exotic particles - WILBs**

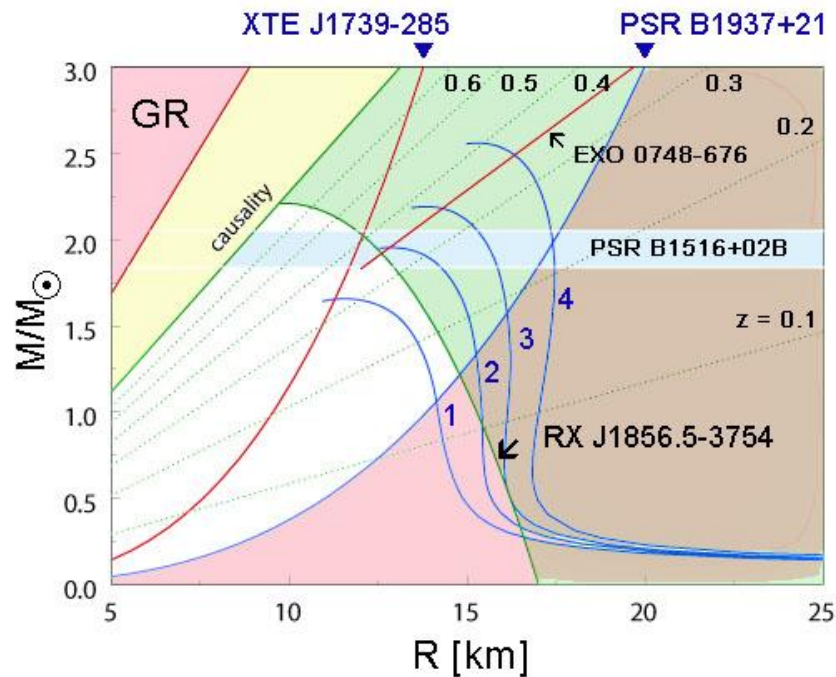
Constraints on the coupling strength with nucleons $g^2/(4\pi)$ and the mass μ (α_G and λ):



- 1 - S. K. Lamoreaux, Phys. Rev. Lett. 78, 5 (1997).
- 2 - R. S. Decca et al., Phys. Rev. Lett. 94, 240401 (2005).
- 3 - V. M. Mostepanenko et al., J. Phys. A41, 164054 (2008).
- 4 - M. Bordag et al., Phys. Lett. A187, 35 (1994).
- 5, 10 - Yu. N. Pokotilovski, Phys. Atom. Nucl. 69, 924 (2006),
R. Barbieri, T. E. O. Ericson, Phys. Lett. B57, 270 (1975)
- 6 - V. V. Nesvizhevsky, G. Pignol, K. V. Protasov, Phys. Rev. D77, 034020 (2008).

POSSIBLE REASONS OF LOW MASSES OF THE HYPERON STARS:

1. Inadequacy of OBE models of nuclear matter at high densities
2. Poor knowledge of the interaction forces between hyperons
3. **Missing contribution of new exotic particles - WILBs**



Neutron stars with WILBs:

D. H. Wen, B. A. Li, and L. W. Chen,

PRL 103, 211102 (2009).

M.I.K., F. Simkovic, A. Faessler,

PRD 79, 125023 (2009).

POSSIBLE REASONS OF LOW MASSES OF THE HYPERON STARS:

1. Inadequacy of OBE models of nuclear matter at high densities
2. Poor knowledge of the interaction forces between hyperons
3. Missing contribution of new exotic particles - WILBs

What about EoS in *s*-channel exchange models?

REMARK ABOUT EXOTIC STATES OF NUCLEAR MATTER:

Vol 441|29 June 2006|doi:10.1038/nature04858

nature

LETTERS

Soft equations of state for neutron-star matter ruled out by EXO 0748–676

F. Özel¹

precision². Here I report a determination of the mass and radius of the neutron star EXO 0748–676 that appears to rule out all the soft equations of state of neutron-star matter. If this object is typical, then condensates² and unconfined quarks¹ do not exist in the centres of neutron stars.

**In MF new degrees of freedom
soften EoS**

Beyond MF this is not true:

Amand Faessler, A.J. Buchmann, M.I.K., *Phys. Rev. C* 56, 1576 (1997)

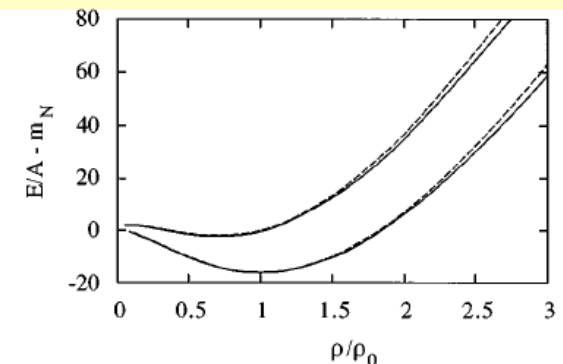


FIG. 2. Saturation curve for nuclear matter in the RHA: without dibaryons (solid line) and with the inclusion of H dibaryons (dashed line) for $h_\sigma/(2g_\sigma) = 0.6$.

INTRODUCTION

$$A(s,t) = \sum_R \text{[Diagram R]} = \sum_P \text{[Diagram P]}$$

What about EoS in *s*-channel exchange models?

INTRODUCTION - HISTORY

$$A(s,t) = \sum_R \text{[Diagram R]} = \sum_P \text{[Diagram P]}$$

- **Analyticity and unitarity for amplitudes lead to the Low scattering equation**
Low (1955)
- **CDD poles as ambiguities in solutions to the Low scattering equation - Castillejo, Dalitz, Dyson (1956)**

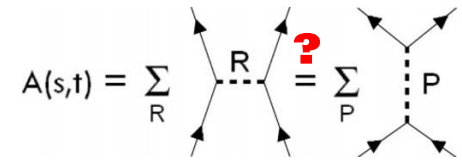
Д. В. ШИРКОВ, В. В. СЕРЕБРЯКОВ, В. А. МЕЩЕРЯКОВ

ДИСПЕРСИОННЫЕ ТЕОРИИ
СИЛЬНЫХ ВЗАИМОДЕЙСТВИЙ
ПРИ НИЗКИХ ЭНЕРГИЯХ

12.1. Модель Дайсона. Физический смысл членов КДЦ.

- **To clarify the physical meaning of the CDD poles, Dyson constructed a model that demonstrates the relationship of the CDD poles to bound states and resonances**
Dyson (1957)

INTRODUCTION - HISTORY

$$A(s,t) = \sum_R \text{[Diagram R]} = \sum_P \text{[Diagram P]}$$


- **Analyticity and unitarity for amplitudes lead to the Low scattering equation**
Low (1955)
- **CDD poles as ambiguities in solutions to the Low scattering equation - Castillejo, Dalitz, Dyson (1956)**
 - **To clarify the physical meaning of the CDD poles, Dyson constructed a model that demonstrates the relationship of the CDD poles to bound states and resonances**
Dyson (1957)

INTRODUCTION - HISTORY

$$A(s,t) = \sum_R \text{[Diagram with R and a red question mark]} = \sum_P \text{[Diagram with P]}$$

- **Analyticity and unitarity for amplitudes lead to the Low scattering equation**
Low (1955)
- **CDD poles as ambiguities in solutions to the Low scattering equation - Castillejo, Dalitz, Dyson (1956)**
- **To clarify the physical meaning of the CDD poles, Dyson constructed a model that demonstrates the relationship of the CDD poles to bound states and resonances**

Dyson (1957)

**Lee-Dyson model
is a model for systems
with **ATTRACTION****

where is

REPULSION?

INTRODUCTION - HISTORY

$$A(s,t) = \sum_R \text{[diagram with R]} = \sum_P \text{[diagram with P]}$$

The diagram shows the equality of two sums. The left sum is over states R, with a diagram of four external lines meeting at a central point via a dashed line labeled R. A red question mark is placed above the dashed line. The right sum is over states P, with a diagram of four external lines meeting at a central point via a dashed line labeled P.

- P matrix method for identifying exotic multiquark states with **PRIMITIVES** «элементарный» that appear as poles of the P matrix

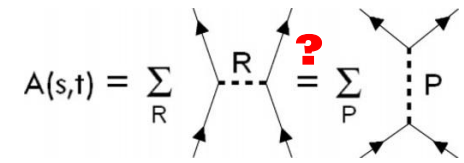
$$P = kb \cot[kb + \delta(s)]$$

rather than the S matrix:

$$S = e^{2i\delta(s)} = \frac{D(s - i0)}{D(s + i0)}$$

Jaffe and Low (1979)

INTRODUCTION - HISTORY

$$A(s,t) = \sum_R \text{diagram}_R = \sum_P \text{diagram}_P$$


- P matrix method for identifying exotic multiquark states with **PRIMITIVES** «элементарный» that appear as poles of the P matrix

$$P = kb \cot[kb + \delta(s)]$$

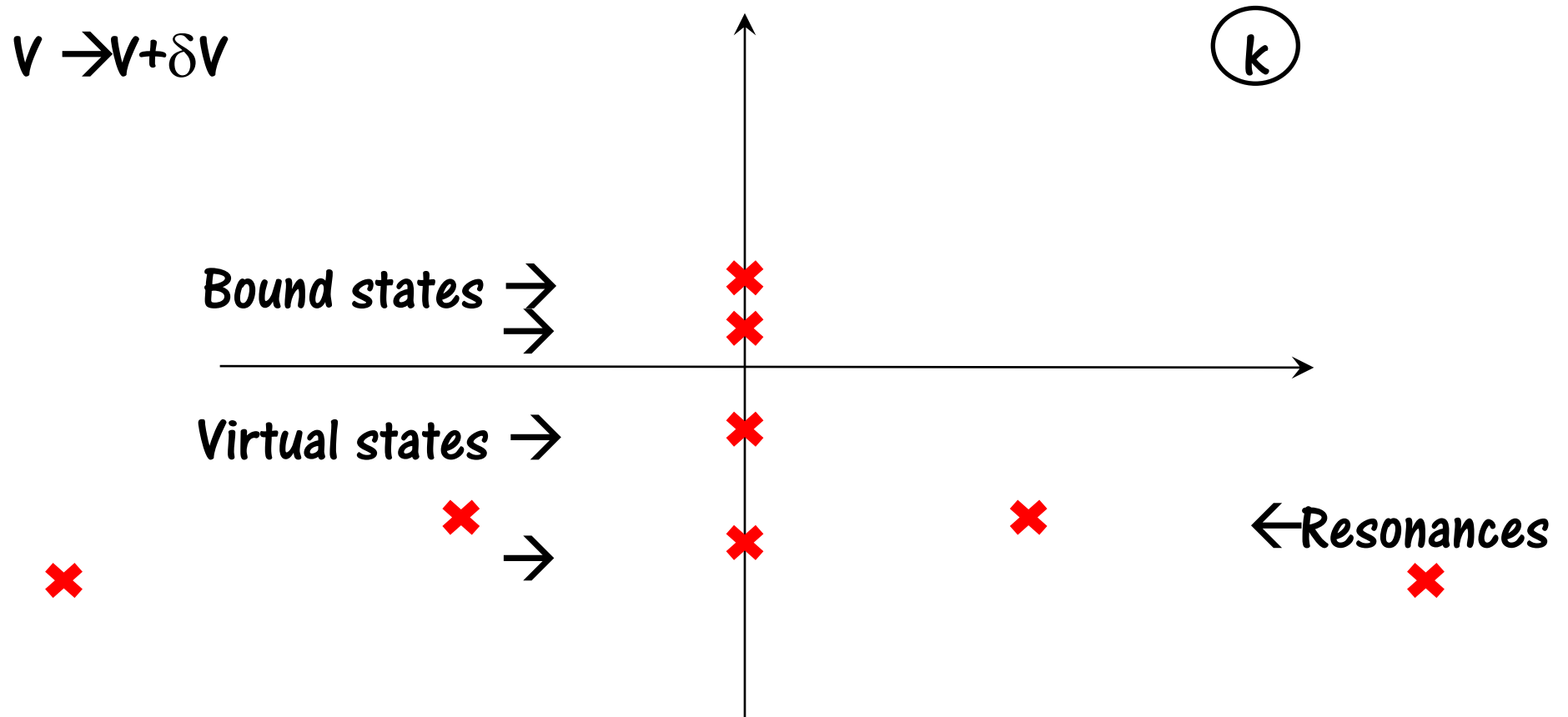
rather than the S matrix:

$$S = e^{2i\delta(s)} = \frac{D(s - i0)}{D(s + i0)}$$

Jaffe and Low (1979)

Physical meaning of primitives?

S-matrix poles in t- and s-channel exchange models

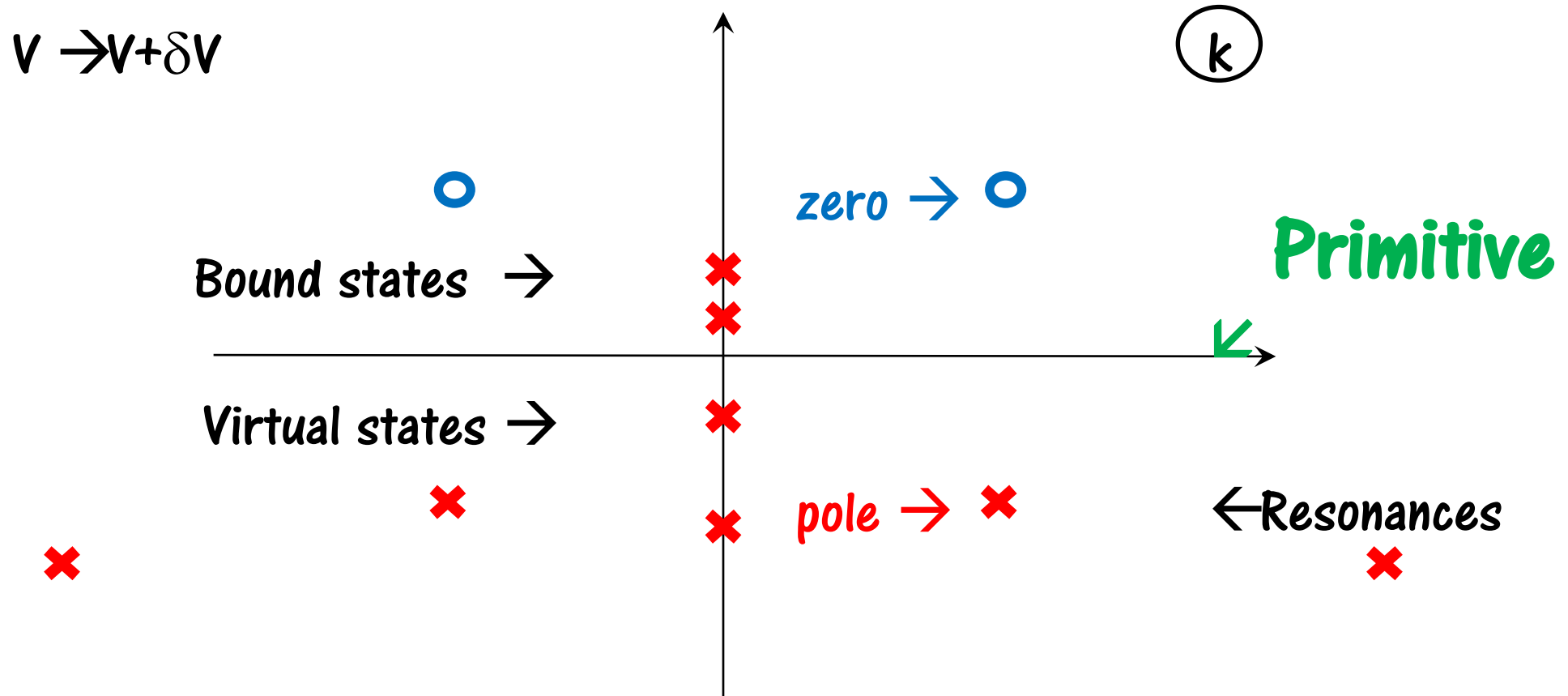


Bound states - Virtual states - Resonances conversion

**e.g. Hydrogen atom
in electric field**

**Increased $g_{\pi NN}$
in the $pp\ ^1S_0$ channel**

S -matrix poles and zeros in s -channel exchange model

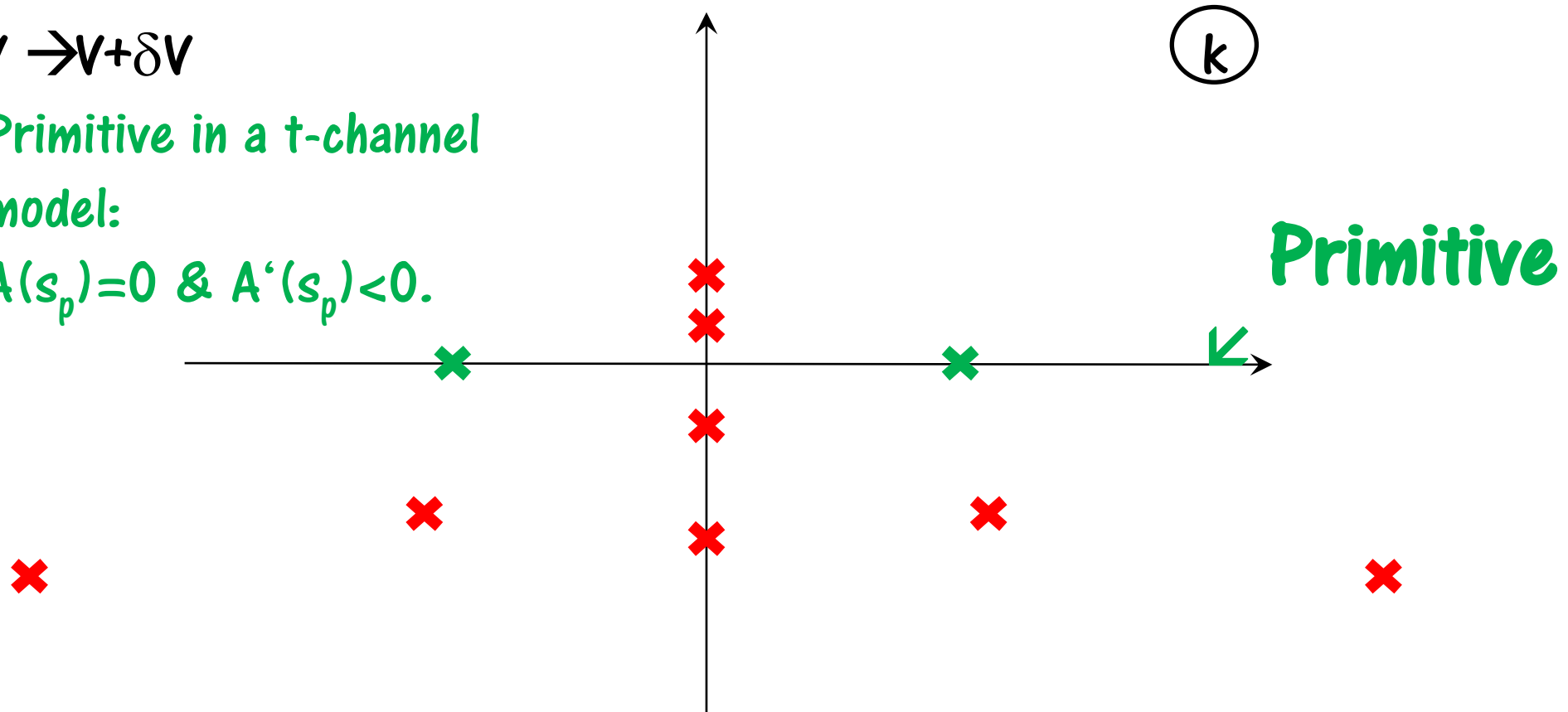


S-matrix poles, zeros and a primitive in a t-channel exchange model

$$V \rightarrow V + \delta V$$

Primitive in a t-channel
model:

$$A(s_p) = 0 \text{ \& \ } A'(s_p) < 0.$$

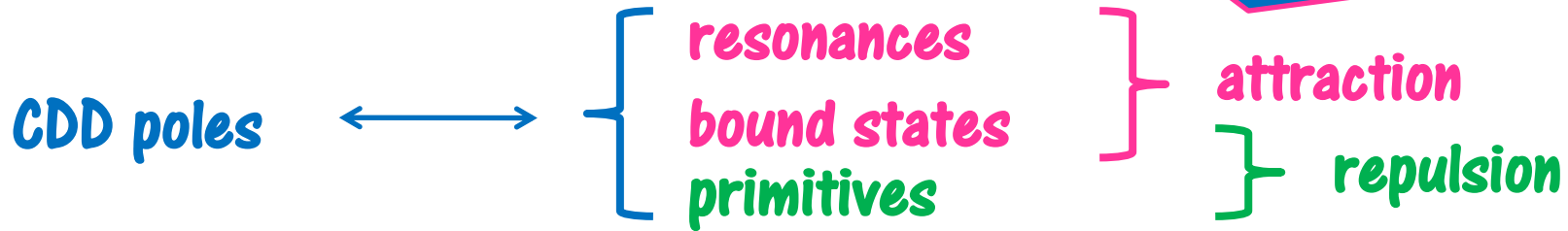


The same old Bound states- Virtual states- Resonances conversion
but primitives do not mix ..

P matrix method for identifying exotic multiquark states with primitives

that appear as poles of the P matrix rather than the S matrix:

Jaffe and Low (1979)



QCB model

A dynamical model of the P matrix was developed and applied to the description of NN scattering

Simonov (1981)

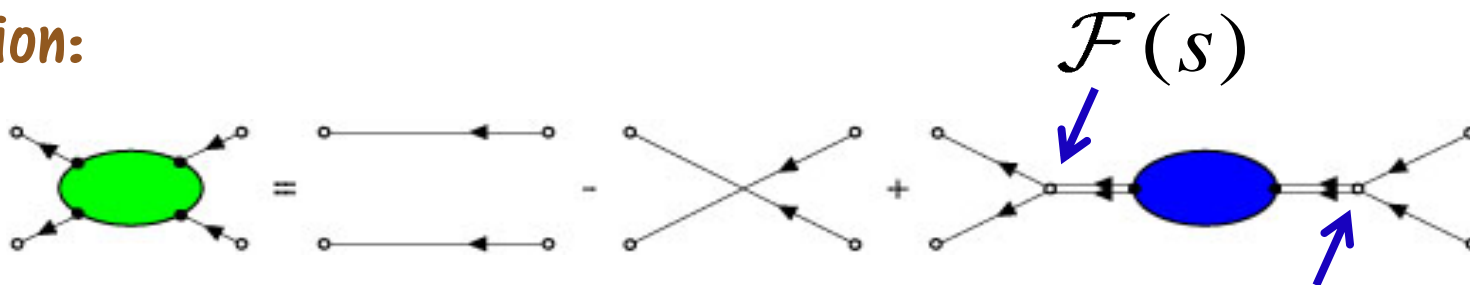
CDD poles correspond to resonances, bound states, and primitives

QCB model through diagrams

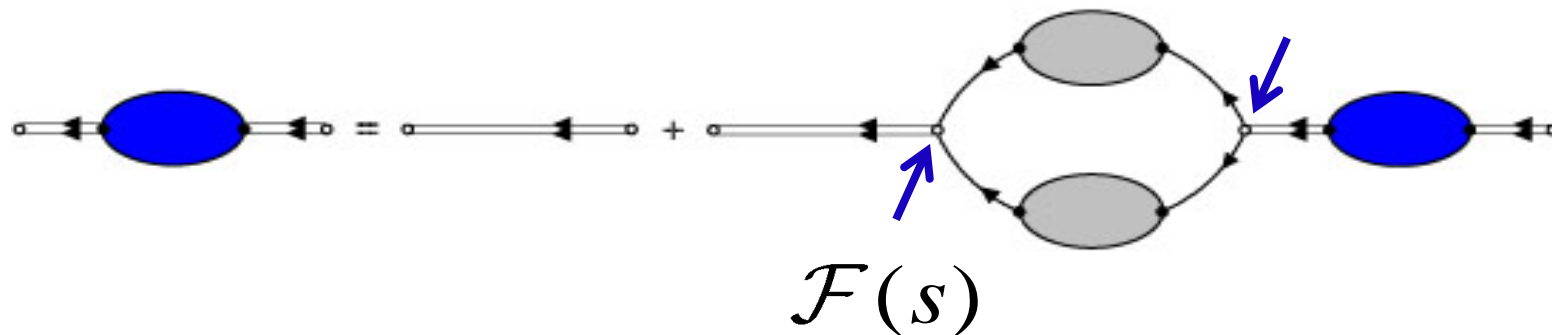
$$A(s,t) = \sum_R \text{diagram with R} = \sum_P \text{diagram with P}$$

Two-body SCATTERING:

The 2-body Green's function:



Compound state propagator:



Analyticity = Yes, elastic unitarity = Yes, crossing symmetry = No

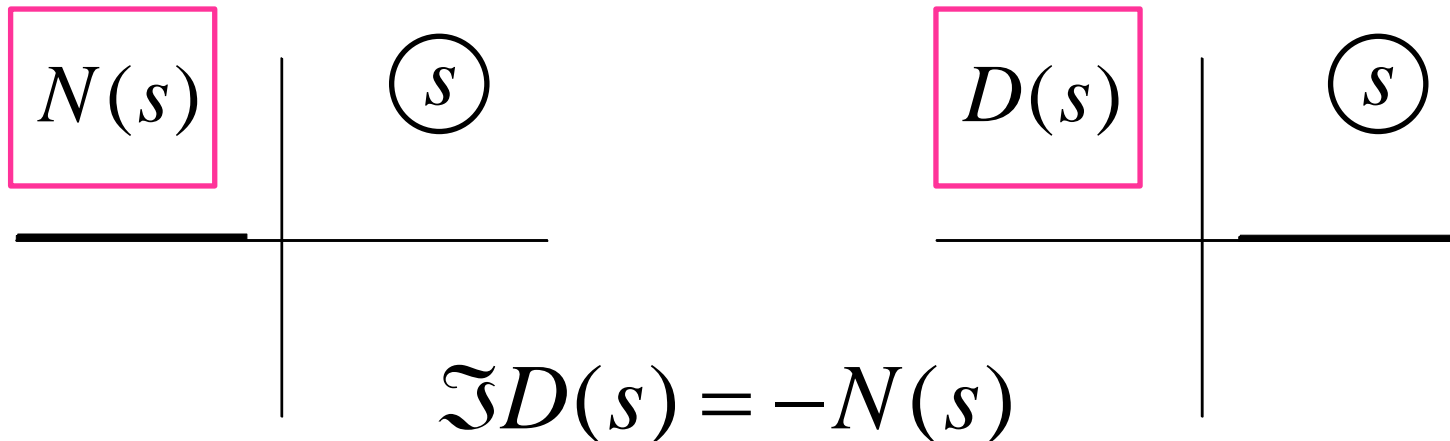
QCB model through diagrams

$$A(s,t) = \sum_R \text{[Diagram R]} = \sum_P \text{[Diagram P]}$$

One starts from the scattering of two particles, e.g., a nucleon and a pion. A nucleon can absorb a pion and can turn into an excited compound state.

The scattering amplitude

$$A(s) \equiv e^{i\delta(s)} \sin \delta(s) = \frac{N(s)}{D(s)}.$$



from unitarity

QCB model through diagrams

$$A(s,t) = \sum_R \text{[Diagram R]} = \sum_P \text{[Diagram P]}$$

D function of the process: $\rightsquigarrow s - M^2 + iM\Gamma$

$$D(s) = \Lambda(s) - \Pi(s),$$

where, in the relativistic $\{tg\}$ notations,

The poles of $\Lambda(s)$ are the CDD poles

$$\Lambda^{-1}(s) = \sum_{\alpha} \frac{g_{\alpha}^2}{s - M_{\alpha}^2} \rightarrow \text{Masses of compound states}$$

$\{ctg\}$

$$\Pi(s) = \frac{1}{\pi} \int_{s_0}^{+\infty} \frac{N(s')}{s' - s} ds',$$

$$N(s) = -\Phi_2(s) \mathcal{F}^2(s).$$

\rightsquigarrow phase space



QCB model through diagrams

$$A(s,t) = \sum_R \text{[diagram with R]} = \sum_P \text{[diagram with P]}$$

The **D** function constructed in such a way is the generalized **R** function. The **S** matrix has the form

$$S = e^{2i\delta(s)} = \frac{D(s - i0)}{D(s + i0)}.$$

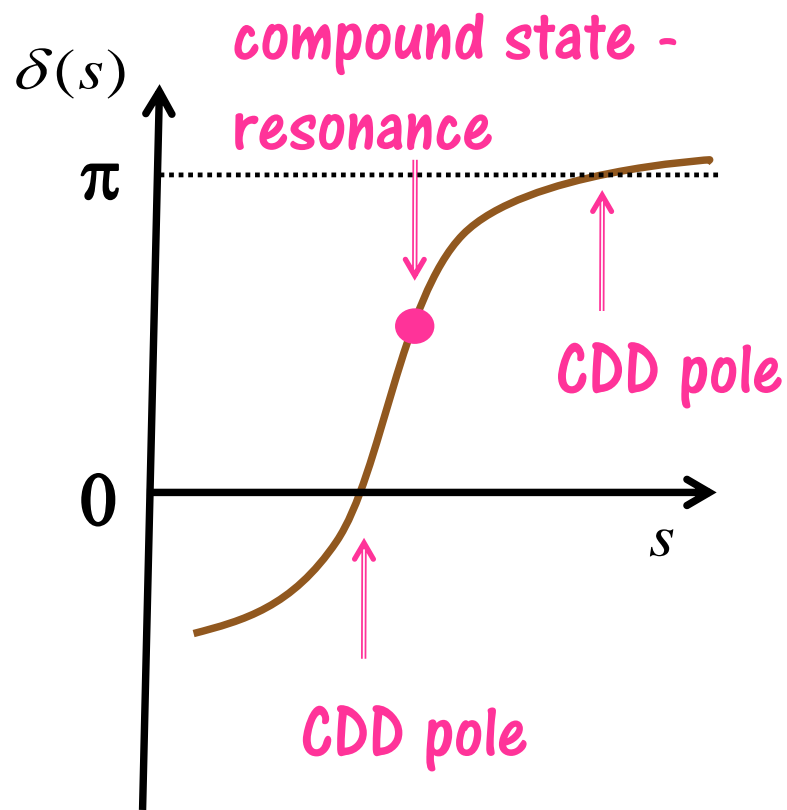
At the **CDD poles** $s = s_\gamma$

$$\delta(s) = 0 \pmod{\pi},$$

the slope of the phase is positive. By expanding the D function around $s = s_\gamma$, one finds

$$\delta(s_\gamma)' = \underbrace{-\Im D(s_\gamma)}_{> 0} \underbrace{\Lambda^{-1}(s_\gamma)'}_{< 0} > 0.$$

The Dyson model applies to systems with attraction where scattering phase shifts increase with increasing energy



Resonances drive the phase shift up

CDD pole = zero phase with a positive slope

QCB model through diagrams

$$A(s,t) = \sum_R \text{[Diagram R]} = \sum_P \text{[Diagram P]}$$

The nucleon-nucleon phase shifts, conversely, decrease with increasing energy and provide evidence for a repulsion.

Low (1955)

Castillejo, Dalitz, Dyson (1956)

Dyson (1957)

$$\Im D(s) > 0$$

attraction

Simonov (1981)

$$\Im D(s) \geq 0$$

attraction & repulsion

$$\exists s_p : \mathcal{F}(s_p) = 0$$

$$\Im D(s) = \Phi_2(s) \mathcal{F}^2(s)$$

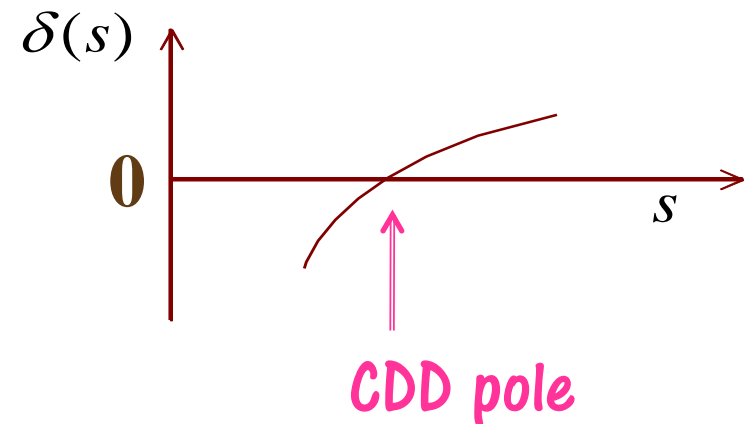
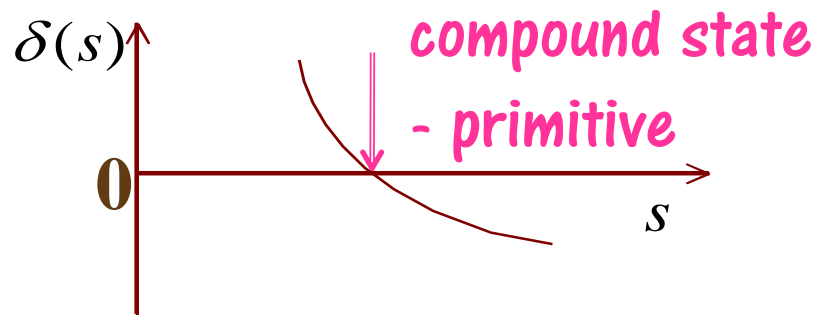
If $D(s_p) = 0$ for real $s_p \in (s_0, +\infty)$, the phase crosses the level

$$\delta(s) = 0 \pmod{\pi},$$

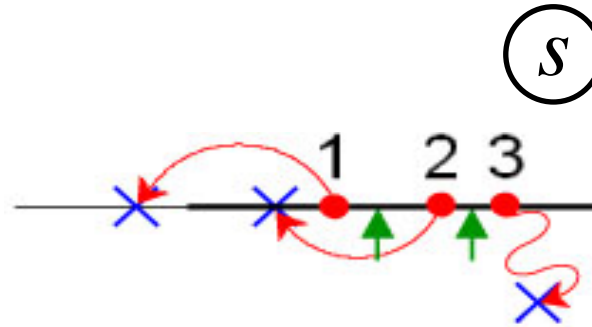
with a negative slope. This can be verified by expanding $D(s)$ around s_p :

$$\delta(s_p)' = -\frac{\Im D(s_p)''}{2\Re D(s_p)'} < 0.$$

In potential scattering, a negative slope of the phase shift is associated with a repulsion



D-FUNCTION ZEROS IN THE COMPLEX s -PLANE



Compound states 1, 2, and 3 move to new positions:
bound state, primitive, and resonance.

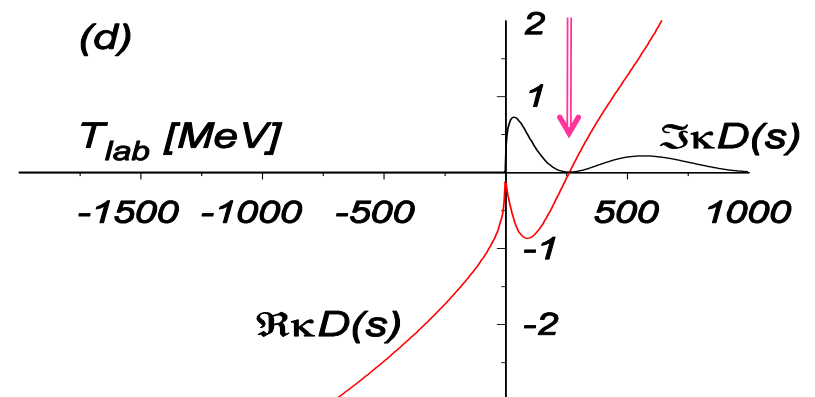
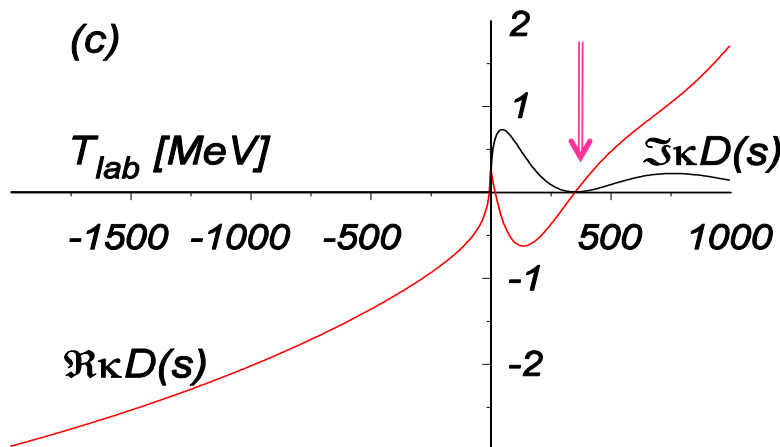
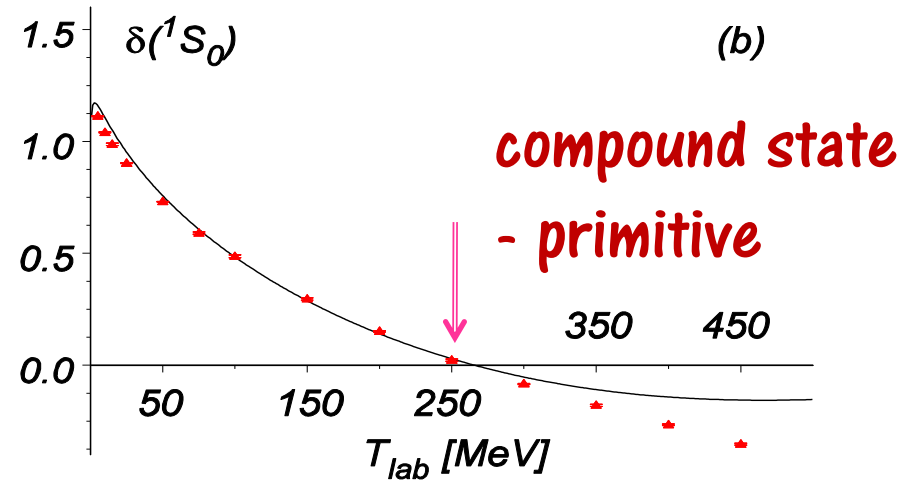
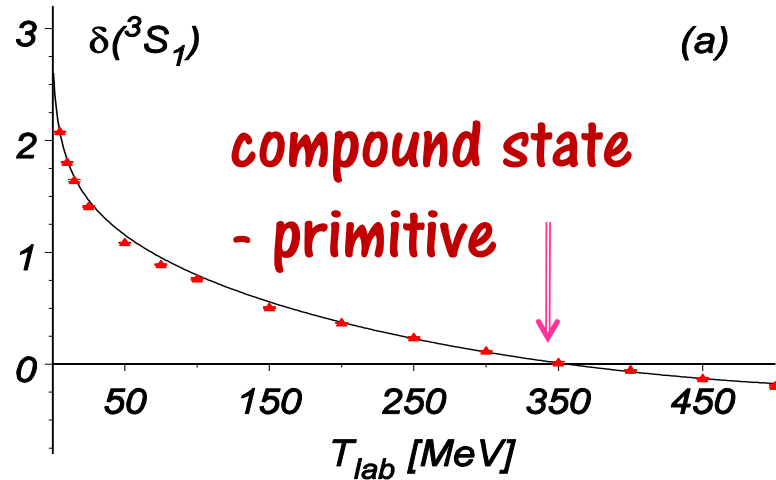
A pair of the CDD poles that squeezes compound state 2 of the primitive type is shown by arrows.

QCB model applies to systems with attraction and repulsion

NN scattering S -wave phase shifts and D functions versus the proton kinetic energy

$$A(s,t) = \sum_R \text{[Diagram R]} = \sum_P \text{[Diagram P]}$$

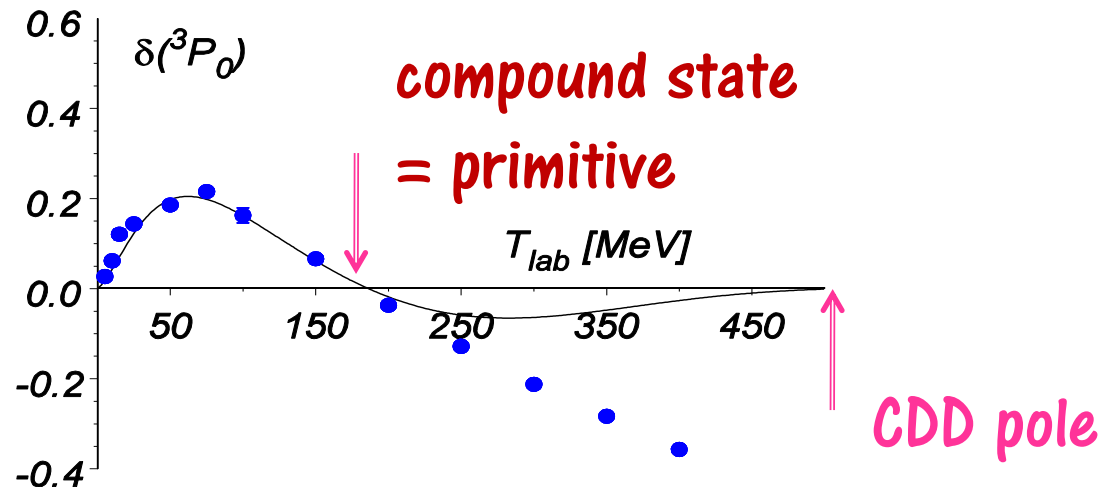
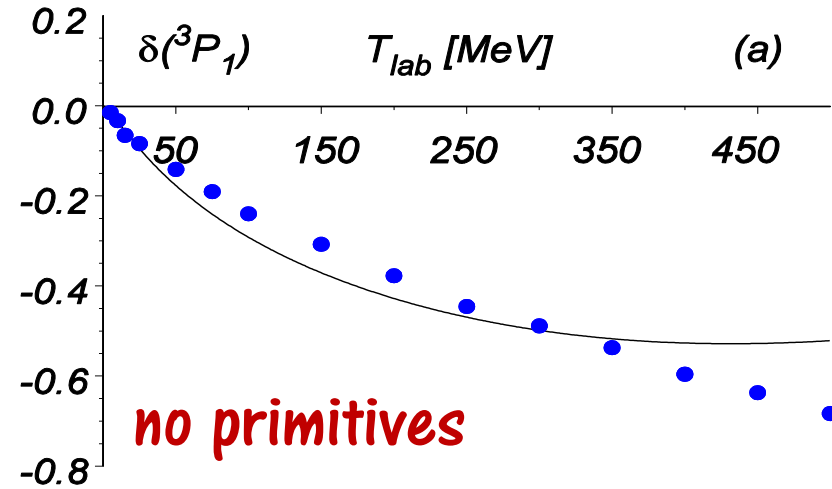
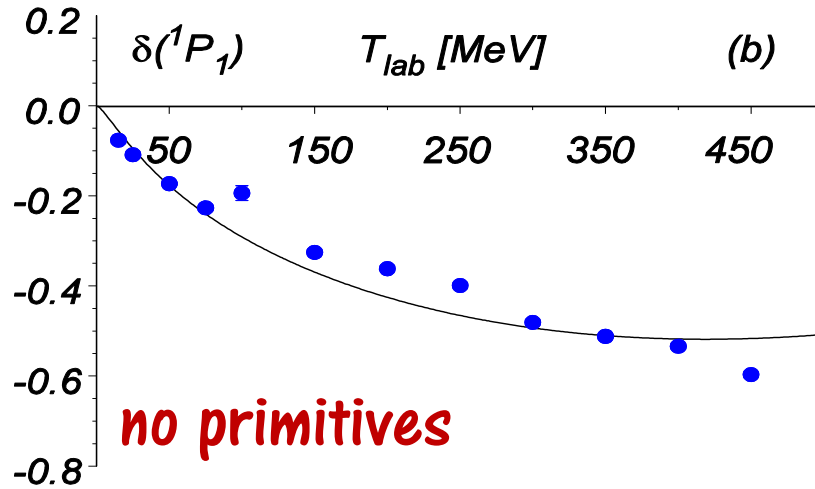
The diagram shows two Feynman-like diagrams for scattering. The left diagram, labeled 'R', shows an incoming particle from the left and an outgoing particle to the right, with a dashed line representing a resonance state. A red question mark is placed above this diagram. The right diagram, labeled 'P', shows an incoming particle from the left and an outgoing particle to the right, with a dashed line representing a pole state.



NN scattering P-wave phase shifts versus the proton kinetic energy

$$A(s,t) = \sum_R \text{[Diagram R]} = \sum_P \text{[Diagram P]}$$

The diagram shows two Feynman-like diagrams for scattering. The left diagram, labeled 'R', shows two incoming particles from the left and two outgoing particles to the right, with a dashed line representing a resonance between them. A red question mark is placed above this diagram. The right diagram, labeled 'P', shows two incoming particles from the left and two outgoing particles to the right, with a dashed line representing a pole between them.



The generalized Low scattering equation

$$A(s,t) = \sum_R \text{[Diagram R]} = \sum_P \text{[Diagram P]}$$

The scattering amplitude

$$A(s) \equiv e^{i\delta(s)} \sin \delta(s) = -\frac{\Phi_2(s)\mathcal{F}^2(s)}{D(s)}$$

obeys the generalized Low scattering equation

$$\frac{A(s)}{\Phi_2(s)\mathcal{F}^2(s)} = \frac{1}{\pi} \int_{s_0}^{+\infty} \frac{|A(s')|^2}{\Phi_2(s')\mathcal{F}^2(s')} \frac{ds'}{s'-s} - \sum_b \frac{C_b}{s-s_b} - \sum_p \frac{C_p}{s-s_p} - C$$

NEW

$\sum_p \frac{C_p}{s-s_p}$

$s_b < s_0 < s_p$

(Intermediate) Summary

$$A(s,t) = \sum_R \text{[Diagram with R]} = \sum_P \text{[Diagram with P]}$$

- The CDD poles are related to **bound states, resonances**, and **primitives**.

- **New primitive-type CDD poles occur**

- In the 3S_1 , 1S_0 and 3P_0 NN channels,

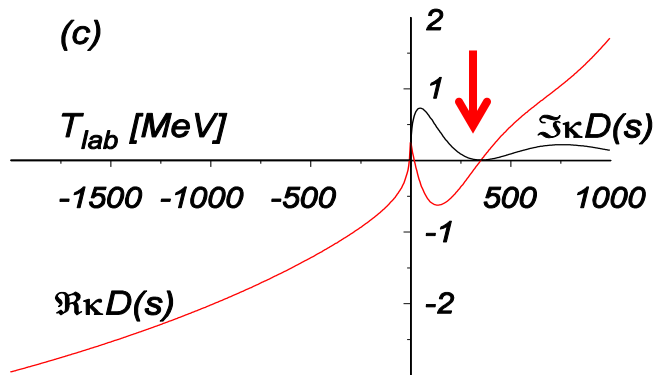
the CDD poles at $M = 3203, 2916,$ and 2650 MeV are associated with the **primitives** at **2047, 2006, and 1969** MeV, respectively.

of our interest -- **how to detect it?**



QCB model for strong & electromagnetic interactions

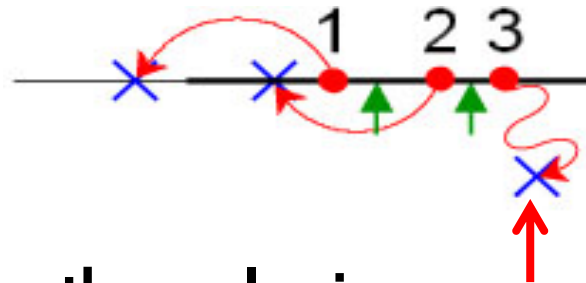
ASSUMING THAT IN THE BARE STRONG INTERACTION
i.e. FOR $\alpha = 1/137 \rightarrow 0$ THE ROOT OF EQUATION



$$D(s) = 0$$

LIES ON THE REAL AXIS:

FIND THE EFFECT OF $\alpha = 1/137 \neq 0$



The root of $D(s)$ will move away from the real axis,

TURNING PRIMITIVE TO A RESONANCE

QCB model for strong & electromagnetic interactions

D function

$$A(s) = N(s)/D(s) \text{ \& } \text{Im}D(s) = -N(s)$$

$$D(s) = \Lambda(s) - \Pi(s),$$

with

$$\Lambda^{-1}(s) = \sum_{\beta} \frac{g_{\beta}^2}{s - M_{\beta}^2} + f, \quad \rightarrow \text{4-fermion interaction}$$

$$\Pi(s) = -\frac{1}{\pi} \int_{s_0}^{+\infty} \Phi_2(s') \frac{\mathcal{F}^2(s')}{s' - s} ds'.$$

In the pp channel the form factor is modified:

$$\mathcal{F}(s) = \left(\frac{s}{s_0} \right)^{1/4} \frac{\sin(kb)}{kb} C_0(s),$$

where $C_0(s)$ is the Gamow-Sommerfeld factor

$$C_0^2(k) = \frac{2\pi\eta}{\exp(2\pi\eta) - 1}, \quad \text{with} \quad \eta = \frac{\alpha\mu}{k}.$$

QCB model for strong & electromagnetic interactions

The dispersion integral can be evaluated to give

$$\kappa\Pi(s) = \frac{1}{2k^2b} \left(2\text{Si}(2kb) \sin(2kb) + (\text{Ci}(2kb) + \text{Ci}(-2kb)) \cos(2kb) - 2C - \ln(-4k^2b^2) \right) - \frac{\sin(kb)}{kb} e^{ikb} \left(C_0^2(k) + \frac{\pi}{k} \right) + \sum_{n=1}^{\infty} \frac{\sinh(b/n)}{b/n} e^{-b/n} \frac{2}{1+k^2n^2},$$

where $\kappa = 2mb/\pi$ in units $\alpha\mu = 1$.

$\Lambda^{-1}(s)$ has a single pole corresponding to a 6q-compound state

$$\kappa^{-1}\Lambda^{-1}(s) = c_p \left(\frac{r_p}{s - M^2} - \frac{r_p}{s_0 - M^2} \right) - \frac{1}{\gamma},$$

with

$$\kappa c_p r_p = g_1^2, \quad r_p = 8\pi^2 / b^2, \quad c_p r_p = \xi \frac{M^2 - s_0}{\gamma}, \quad \xi \in (0, 1).$$

coupling with continuum

residue of the free P matrix

analyticity of D funct.

QCB model for strong & electromagnetic interactions

In the pp channel, we use the series expansion around $k = 0$

Bethe (1949)

$$kC_0^2(s) \cot \delta(k) + 2h(k) = \frac{1}{a} + \frac{r}{2}k^2 + \dots,$$

where $h(k)$ is defined by

$$2\psi\left(1 + \frac{i}{k}\right) + ik + \ln(-k^2) = 2h(k) + ikC_0^2(s).$$

γ is determined by the scattering length, the effective range is predicted:

$$\gamma = 1 + \frac{b}{a} + \left(\ln(4b^2) + 4C - 3\right)b - \sum_{m=2}^{\infty} (-1)^m \frac{2^{m+1}}{(m+1)!} b^m \zeta(m),$$

$$r = \frac{2}{3}(1 + \gamma)b - \frac{8\gamma\xi}{b(M^2 - 4m^2)} - \frac{7}{9}b^2 + \sum_{m=2}^{\infty} (-1)^m \frac{2^{m+2}(m-1)(m+6)}{3(m+3)!} b^{m+1} \zeta(m).$$

In the 1S_0 np channel, we obtain $r = 2.1$ fm versus 2.8 fm in OBE models

The zeros of $\text{Im } D(s)$ are the zeros of the phase shift and the zeros of the form factor

$$\mathcal{F}(s) = \left(\frac{s}{s_0} \right)^{1/4} \frac{\sin(kb)}{kb} C_0(s).$$

We thus find $k^*_0 = \pi/b_0$ and the primitive mass

$$M_0 = 2\sqrt{\pi^2 / b_0^2 + m_0^2}.$$

In the strong interaction + QED, the zero of $D(s)$ is shifted due to:

1. $m_0 \rightarrow m = m_0 + \Delta m$ **EM shift of the nucleon mass**
2. $M_0 \rightarrow M = M_0 + \Delta M$ **EM shift of the primitive mass**
3. $b_0 \rightarrow b = b_0 + \Delta b$ **EM shift of the interaction radius**
4. The Coulomb interaction of the protons
5. The scattering length
6. g_1 is hard to control, $\Delta g_1 \rightarrow 0$.

Electromagnetic mass shifts (# 1,2)

Electromagnetic mass splitting of hadrons is attributed to
Coulomb interaction
& **spin-spin interaction of quarks**

$$\Delta\mathcal{M} = c \left\langle \sum_{i<j} e_i e_j \right\rangle + h \left\langle \sum_{i<j} e_i e_j \boldsymbol{\sigma}_i \boldsymbol{\sigma}_j \right\rangle.$$

In octet-baryon isomultiplets, accounting for the fixed mass difference of nonstrange quarks,

$$c = 3.06 \text{ MeV}, h = -1.35 \text{ MeV},$$

according to J. L. Rosner, Phys. Rev. D 57, 4310 (1998).

1. $m_0 \rightarrow m = m_0 + \Delta m$
2. $M_0 \rightarrow M = M_0 + \Delta M$
3. $b_0 \rightarrow b = b_0 + \Delta b$
4. The Coulomb interaction of the protons
5. The scattering length
6. g_1 is hard to control, $\Delta g_1 \rightarrow 0$.

Average values of the spin-isospin operators and electromagnetic mass shifts of the proton, the neutron, and the $6q$ -compound states d^* (2000) with isospin projections $I = +1, 0, -1$ (in MeV).

Hadron	I_3	$\langle \sum_{i<j} e_i e_j \rangle$	$\langle \sum_{i<j} e_i e_j \sigma_i \sigma_j \rangle$	$\Delta \mathcal{M}$
p	$\frac{1}{2}$	0	$\frac{4}{3}$	-1.8
n	$-\frac{1}{2}$	$-\frac{1}{3}$	1	-2.4
d^{*++}	1	1	$-\frac{7}{5}$	5.0
d^{*+}	0	$-\frac{1}{3}$	$\frac{19}{5}$	-6.2
d^{*0}	-1	$\frac{2}{3}$	$-\frac{2}{5}$	-1.5



pp
np
nn

1. $m_0 \rightarrow m = m_0 + \Delta m$
2. $M_0 \rightarrow M = M_0 + \Delta M$
3. $b_0 \rightarrow b = b_0 + \Delta b$
4. The Coulomb interaction of the protons
5. The scattering length
6. g_1 is hard to control, $\Delta g_1 \rightarrow 0$.

Electromagnetic shift of the interaction radius (# 3)

The MIT bag model gives $b \sim R$ and $M \sim R^3$, where R is the radius of the 6-quark bag

$$\frac{\Delta b}{b} = \frac{\Delta M}{3M}.$$

1. $m_0 \rightarrow m = m_0 + \Delta m$
2. $M_0 \rightarrow M = M_0 + \Delta M$
3. $b_0 \rightarrow b = b_0 + \Delta b$
4. The Coulomb interaction of the protons
5. The scattering length
6. g_1 is hard to control, $\Delta g_1 \rightarrow 0$.

Electromagnetic shift of the interaction radius (# 3)

The MIT bag model gives $b \sim R$ and $M \sim R^3$, where R is the radius of the 6-quark bag

$$\frac{\Delta b}{b} = \frac{\Delta M}{3M}.$$

1. $m_0 \rightarrow m = m_0 + \Delta m$
2. $M_0 \rightarrow M = M_0 + \Delta M$
3. $b_0 \rightarrow b = b_0 + \Delta b$
4. The Coulomb interaction of the protons
5. The scattering length
6. g_1 is hard to control, $\Delta g_1 \rightarrow 0$.

Electromagnetic shift of the interaction radius (# 3)

The MIT bag model gives $b \sim R$ and $M \sim R^3$, where R is the radius of the 6-quark bag

$$\frac{\Delta b}{b} = \frac{\Delta M}{3M}.$$

1. $m_0 \rightarrow m = m_0 + \Delta m$
2. $M_0 \rightarrow M = M_0 + \Delta M$
3. $b_0 \rightarrow b = b_0 + \Delta b$
4. The Coulomb interaction of the protons
5. The scattering length
6. g_1 is hard to control, $\Delta g_1 \rightarrow 0$.

Scattering length (# 5) using heuristic arguments:

In the Born approximation,

$$f(\mathbf{q}) = -\frac{\mu}{2\pi} \int d\mathbf{x} e^{-i\mathbf{q}\cdot\mathbf{x}} U(\mathbf{x}).$$

The scattering length is proportional to the averaged interaction potential:

$$a = \lim_{q \rightarrow 0} f(\mathbf{q}) = -\frac{\mu}{2\pi} \int d\mathbf{x} U(\mathbf{x}).$$

Isospin-dependent part of $U(\mathbf{x})$ leads to a difference of scattering lengths in different isospin channels.

Isospin-dependent mass splitting of hadrons is also determined by averaging the electromagnetic potential, although of quarks rather than nucleons.

In any case, the equation

$$a = a_0 + C_2 \Delta M,$$

with $a_0 = 14.45$ fm and $C_2 = -1.45$ fm/MeV, gives scattering lengths

7.3 fm, 23.4 fm, and 16.6 fm

in the $l = +1, 0, -1$ channels, which agrees well with the empirical data.

1. $m_0 \rightarrow m = m_0 + \Delta m$
2. $M_0 \rightarrow M = M_0 + \Delta M$
3. $b_0 \rightarrow b = b_0 + \Delta b$
4. The Coulomb interaction of the protons
5. The scattering length
6. g_1 is hard to control, $\Delta g_1 \rightarrow 0$.

In any case, the equation

$$a = a_0 + C_2 \Delta M,$$

with $a_0 = 14.45$ fm and $C_2 = -1.45$ fm/MeV, gives scattering lengths

7.3 fm, 23.4 fm, and 16.6 fm

in the $l = +1, 0, -1$ channels, which agrees well with the empirical data.

#6: Coupling with the continuum

$\Delta g_1 = 0$ (not modified)

1. $m_0 \rightarrow m = m_0 + \Delta m$
2. $M_0 \rightarrow M = M_0 + \Delta M$
3. $b_0 \rightarrow b = b_0 + \Delta b$
4. The Coulomb interaction of the protons
5. The scattering length
6. g_1 is hard to control, $\Delta g_1 \rightarrow 0$.

How to fix PARAMETERS:

The proton kinetic energy $T_\delta = 244$ MeV \rightarrow a vanishing phase shift.
In the center-of-mass frame, the momentum of the protons

$$k_\delta = \sqrt{mT_\delta / 2}$$

and their total energy

$$M_\delta = \sqrt{2mT_\delta + 4m^2} = 1995 \text{ MeV.}$$

The phase shift vanishes provided that the imaginary part of the D function vanishes $k_\delta b = \pi$, so the interaction radius b is fixed.

The masses of the compound state M_0 and $M = M_0 + \Delta M \approx M_\delta$ are known, so we find the interaction radius b_0 with the electromagnetic interaction switched off with accuracy $O(\Delta M)$.

Summary TABLE

α	Scattering length a	Effective range r	Interaction radius b	Proton mass m	Compound state mass M	Prim/Resonance mass M_*	Prim/Reso. width Γ_*
0	14.45	2.22	1.829	940.1	1998.6	1998.6	0
1/137	6.50	0.84	1.831	938.3	2003.5	2000.5	0.260

The narrow resonance is associated with the complex root of the equation

$$D(M_*^2 - iM_*\Gamma_*) = 0.$$

A primitive root corresponding to $\Gamma_* = 0 \rightarrow$ **bare strong interaction**

A resonance with $\Gamma_* \neq 0$ occurs in the neighborhood of the primitive

\rightarrow **strong interaction + QED**

PRIMITIVE-TO-RESONANCE CONVERSION IN THE 1S_0 pp CHANNEL

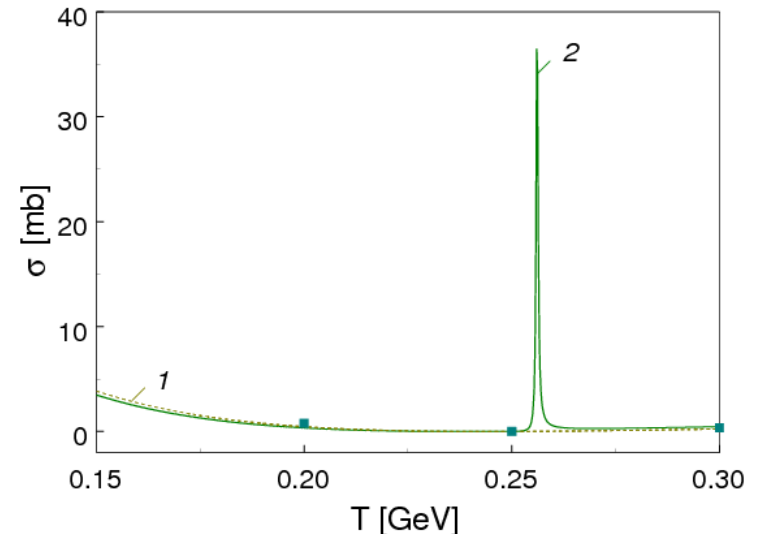
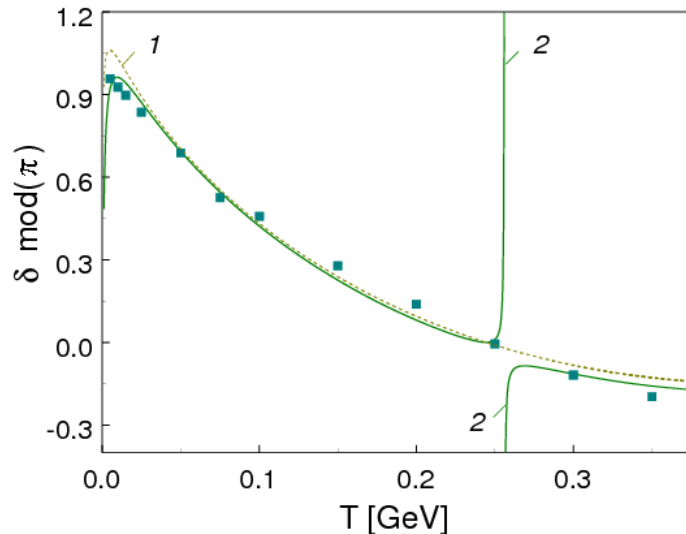
The narrow resonance is associated with the complex root of the equation

$$D(M_*^2 - iM_*\Gamma_*) = 0.$$

A primitive-type root corresponding to $\Gamma_* = 0 \rightarrow$ bare strong interaction

A resonance with $\Gamma_* \neq 0$ occurs in the neighborhood of the primitive

\rightarrow strong interaction + QED



For an experimental search for narrow dibaryon resonances, **one should have a BEAM OF PROTONS**

- *with a kinetic energy of $T \approx 250$ MeV and*
- *an energy spread below 100 keV*

+ HYDROGEN TARGET

The energy resolution of the detector is not important, so one can use cheap scintillation detectors.

In the CELSIUS accelerator at Uppsala,

the beam momentum spread was a few times 10^{-3} before electron cooling

and a few times 10^{-5} after electron cooling.

Under such conditions, it is possible to measure M with an accuracy of **10 keV** or better.

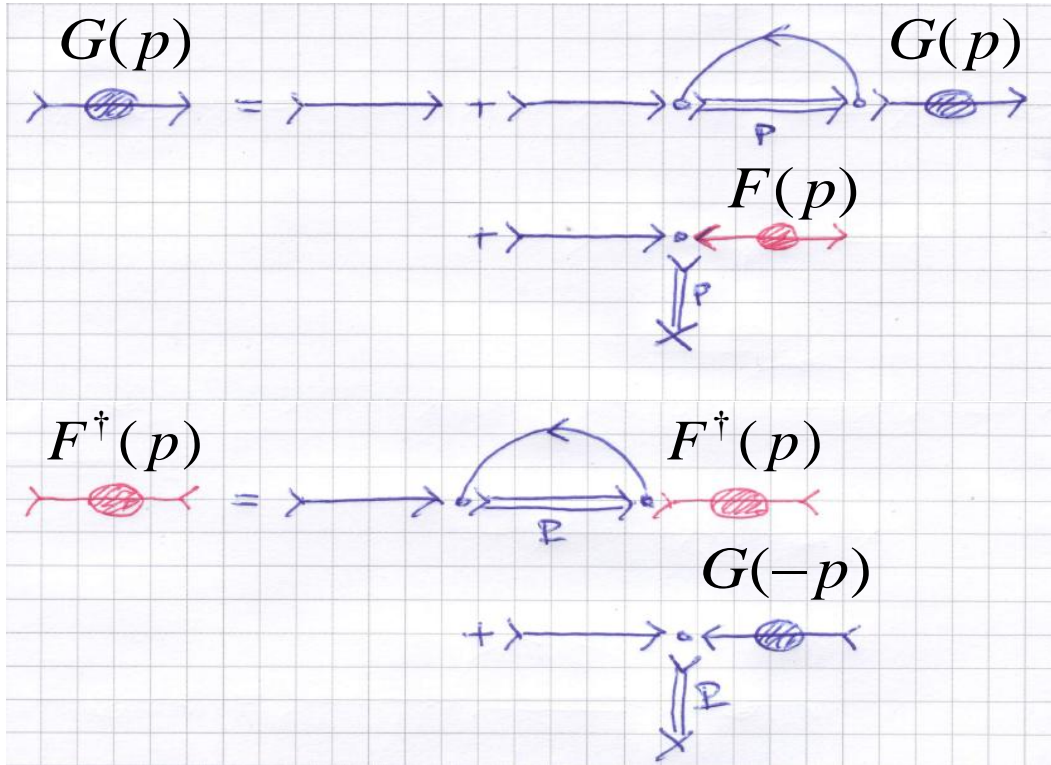
● **The narrow width of $d^*(2000)$ $\Gamma_* = 260$ keV is not an obstacle for its experimental search.**

Neutrons pairing in QCB model

$$A(s,t) = \sum_R \text{diagram} = \sum_P \text{diagram}$$

The diagram shows two equivalent ways to represent the pairing interaction. The first diagram, labeled 'R', shows a dashed line connecting two vertices, with arrows indicating the flow of particles. The second diagram, labeled 'P', shows a similar structure but with a different arrow configuration. A red question mark is placed between the two diagrams.

Уравнения Горькова-Элиашберга



⇒ Green function

NB: очевидное сходство с сепарабельными моделями NN взаимодействий

⇒ anomalous

Green function

GAP Equation:

$$1 = - \int \frac{dp}{(2\pi)^3} \frac{2\pi^2}{E^2(p)} \mathcal{F}(p^2) \Lambda^{-1}(s) \mathcal{F}(p^2) \frac{1}{2\sqrt{(E(p) - \mu)^2 + \Delta^2(s, p)}} \Big|_{s=4\mu^2} .$$

Neutrons pairing in QCB model

$$A(s,t) = \sum_R \text{Diagram with R} = \sum_P \text{Diagram with P}$$

The diagram shows two equivalent ways to represent the function A(s,t). On the left, a central dashed line labeled 'R' is connected to four external lines (two incoming from the left, two outgoing to the right). On the right, a central dashed line labeled 'P' is connected to four external lines (two incoming from the left, two outgoing to the right). A red question mark is placed between the two diagrams, indicating an equivalence or a question about the relationship between the two representations.

Gap

$$\Delta(4\mu^2, \mathbf{p}) = \frac{\sqrt{2}\pi}{E(\mathbf{p})} \mathcal{F}(\mathbf{p}^2) \Lambda^{-1}(4\mu^2) |\Xi|.$$

Condensate

$$i\Xi^* = \int \frac{d^4 p}{(2\pi)^4} \frac{\sqrt{2}\pi}{E(\mathbf{p})} \mathcal{F}(\mathbf{p}^2) F^\dagger(\mathbf{p}),$$

• **Green function:**

$$G(p) = \frac{u_p^2}{\omega - \varepsilon(\mathbf{p}) + i0} + \frac{v_p^2}{\omega + \varepsilon(\mathbf{p}) - i0},$$

$$\begin{pmatrix} u_p^2 \\ v_p^2 \end{pmatrix} = \frac{1}{2} \begin{pmatrix} 1 \pm \frac{\eta_p}{\varepsilon(\mathbf{p})} \end{pmatrix},$$

$$\varepsilon(\mathbf{p}) = \sqrt{\eta_p^2 + \Delta^2(4\mu^2, \mathbf{p})}$$

$$\eta_p = E(\mathbf{p}) - \mu$$

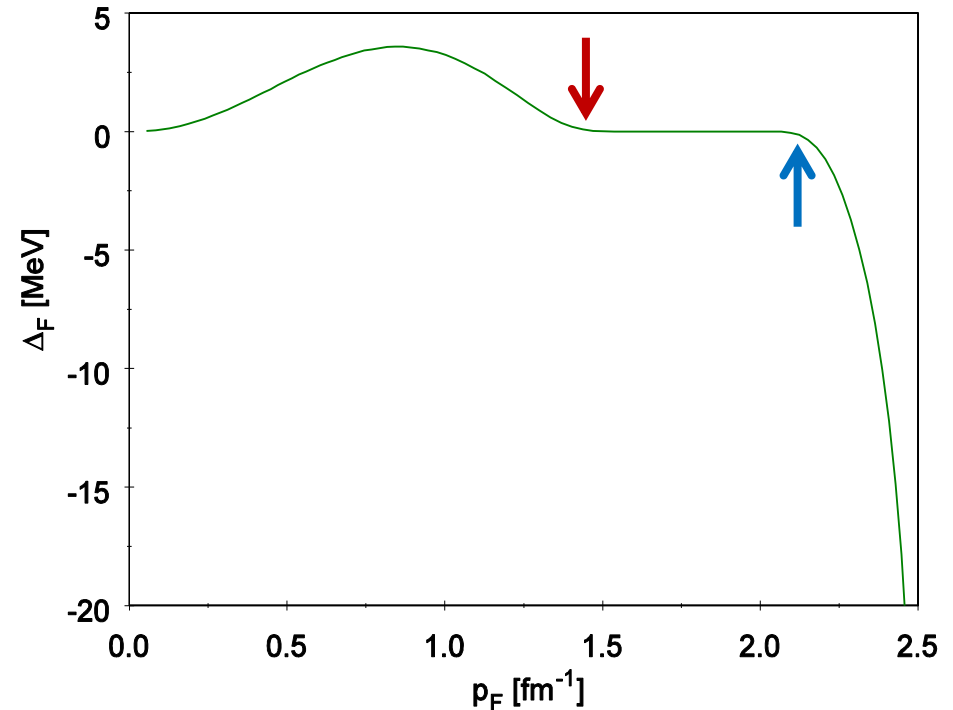
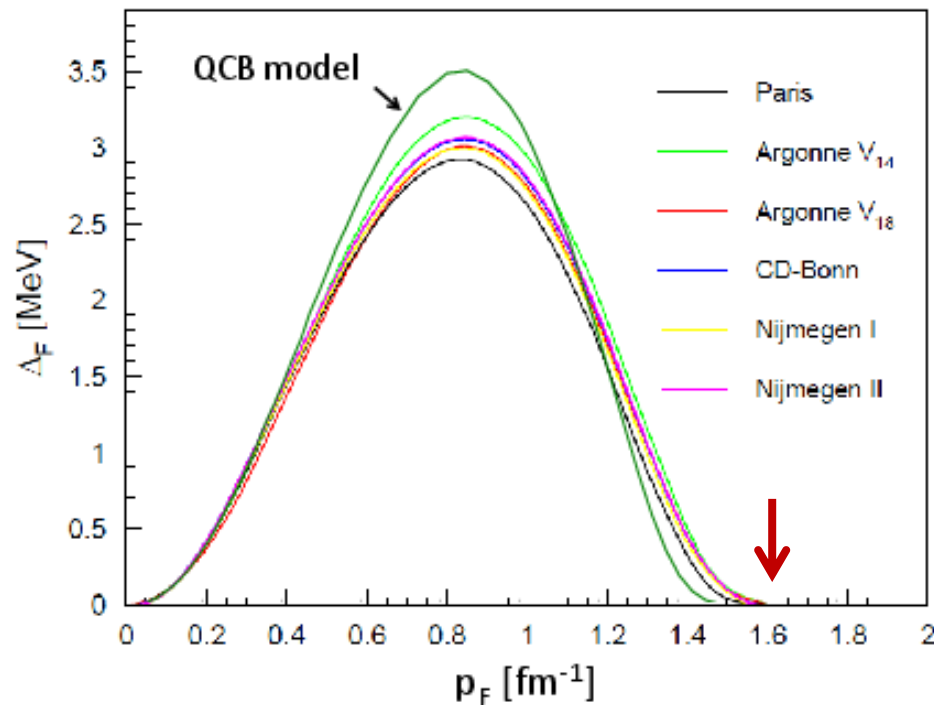
• **Anomalous Green function:**

$$F^\dagger(\mathbf{p}) = -\frac{\sqrt{2}\pi}{E(\mathbf{p})} \mathcal{F}(\mathbf{p}^2) \Lambda^{-1}(4\mu^2) \frac{\Xi^*}{(\omega - \varepsilon(\mathbf{p}) + i0)(\omega + \varepsilon(\mathbf{p}) - i0)}$$

Neutrons pairing in QCB model

$$A(s,t) = \sum_R \text{[diagram with R]} = \sum_P \text{[diagram with P]}$$

Gap vs. p_F in QCB model



**Plotted also are predictions
of t -channel exchange OBE models
Paris, Argonne (2), CD-Bonn, Nijmegen (2)**

**NB: New superconducting phase
of neutron matter
occurs at $p_F > 2 \text{ fm}^{-1}$ (!?)**

If the primitive in high-density nuclear matter turns to a resonance, a dibaryon Bose condensation occurs, which makes neutron stars unstable

A. М. Балдин и др., Доклады Академии Наук СССР 279, 602 (1984).

A. С. Шумовский и В. И. Юкалов, ЭЧАЯ 16, 1274 (1985).

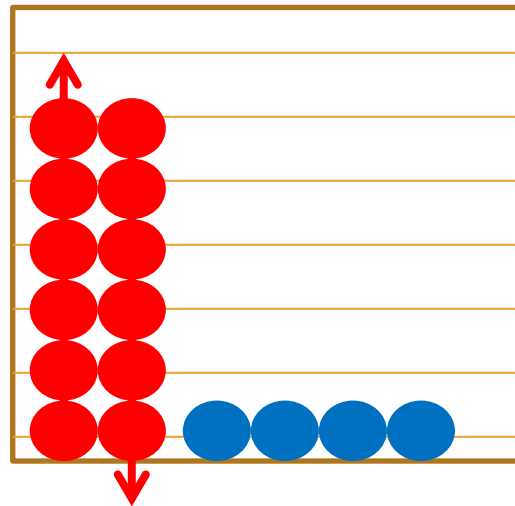
A. V. Chizhov, R. G. Nazmitdinov, A. S. Shumovsky, and V. I. Yukalov, Nucl. Phys. A 449, 660 (1986).

Fermi Energy

$$E_F = m_D/2 \rightarrow$$

Dibaryon

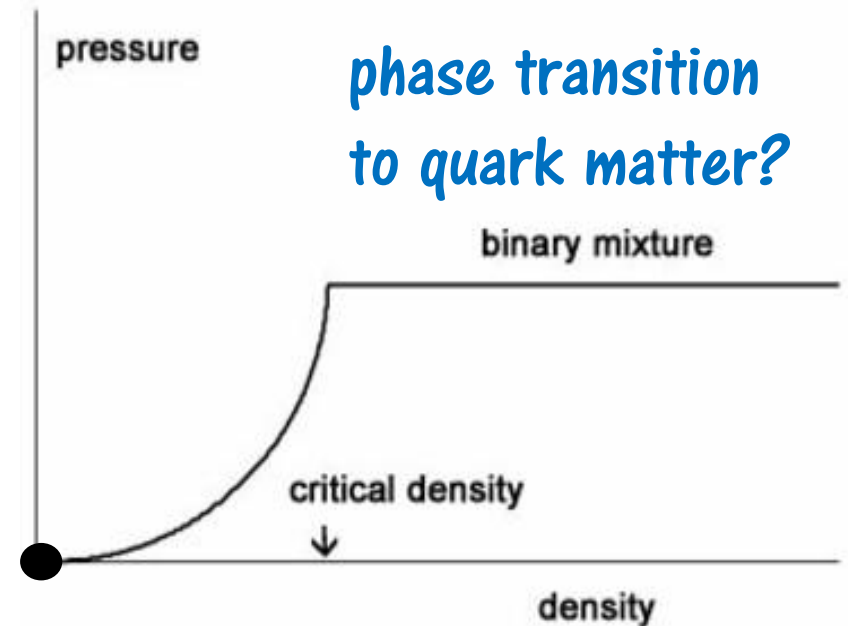
condensate \rightarrow



Euler's equation:

$$\rho \frac{\partial \mathbf{v}}{\partial t} + \rho (\mathbf{v} \cdot \nabla) \mathbf{v} = -\nabla P - \rho \nabla \Phi,$$

М.И.К., Письма ЖЭТФ 46, 5 (1987).

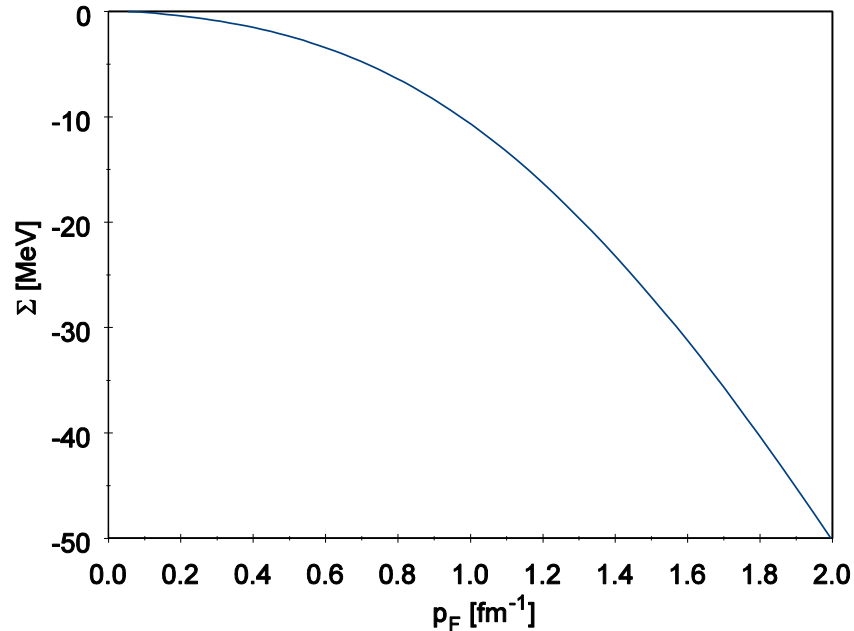


There are no static solutions above the critical density.

EoS in QCB model

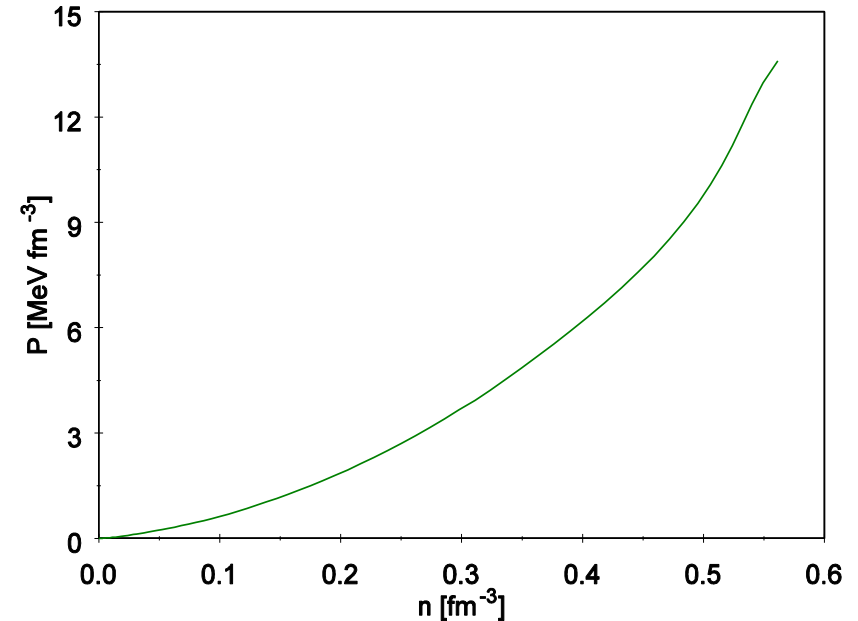
$$A(s,t) = \sum_R \text{[diagram with R]} = \sum_P \text{[diagram with P]}$$

Neutron self-energy vs. p_F



NB: Σ is much smaller than in MF models and comparable with OBE models

Pressure vs. number density

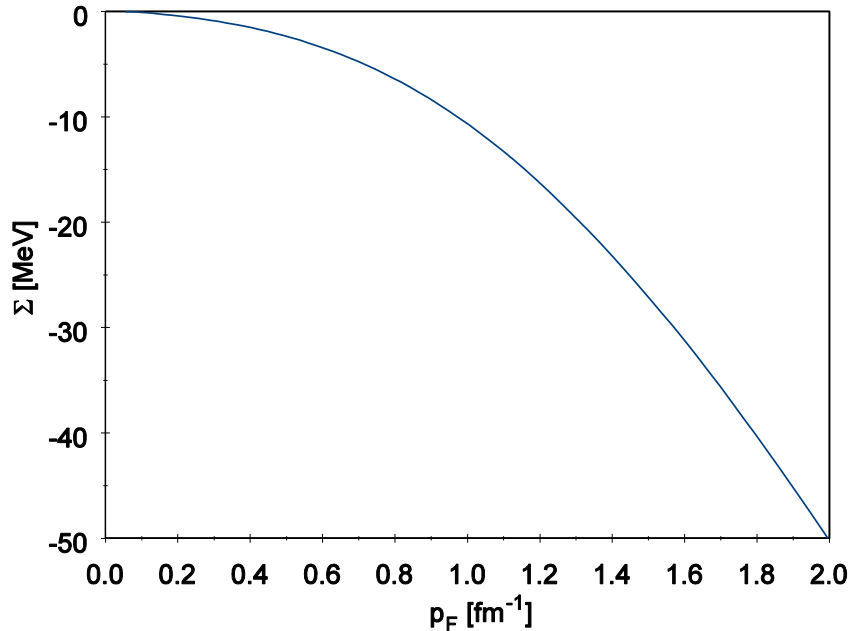


NB: EoS is much softer than in MF models and in OBE models

EoS in QCB model

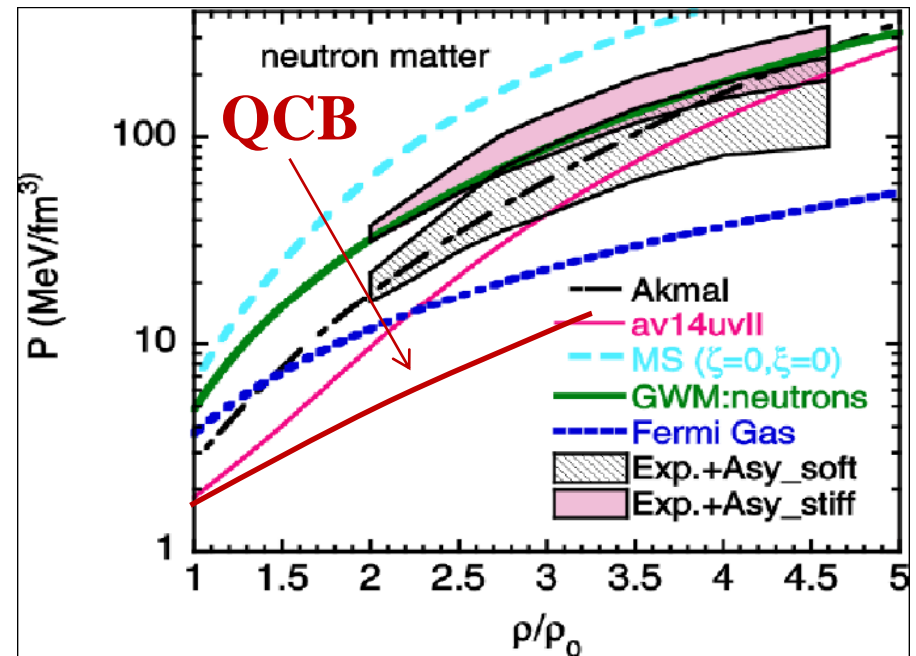
$$A(s,t) = \sum_R \text{[Diagram with R and a red question mark]} = \sum_P \text{[Diagram with P]}$$

Neutron self-energy vs. p_F



NB: Σ is much smaller than in MF models and comparable with OBE models

Pressure vs. number density




EoS for neutron matter in OBE models.
 The dashed regions correspond to the pressure consistent with the experimental flow data in heavy-ion collisions after inclusion of the stiffest and softest asymmetry terms.

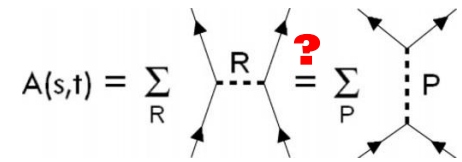
EoS in QCB model

$$A(s,t) = \sum_R \text{[Diagram R]} = \sum_P \text{[Diagram P]}$$

WHAT ELSE COULD BE DONE?

1. Include data on the NN scattering phases up to $T_{\text{lab}} = 500$ MeV 
2. Include NN channels with p - and d -waves
3. Include NN^* and $N\Delta$ channels (not a problem for separable-like potentials)
4. *Exact solution of Eliashberg equations for the pairing*
5. Symmetric nuclear matter at saturation
6. Do primitives stay always on the unitary cut? Duality?
7. A VERY HIGH-DENSITY EOS

SUMMARY

$$A(s,t) = \sum_R \text{[Diagram R]} = \sum_P \text{[Diagram P]}$$


First calculation of EoS of nuclear matter in an s -channel exchange NN interaction model

- The CDD poles are related to **bound states, resonances**
and **PRIMITIVES**
- Primitives are identified reliably
in the 3S_1 , 1S_0 and 3P_0 NN scattering channels
- **Narrow dibaryon resonances $\Gamma \sim 260$ keV**
in the 3S_1 , 1S_0 and 3P_0 NN scattering channels
due to possible **primitive-to-resonance conversion**
- Neutrons pairing in QCB model is well described
- EoS of neutron matter in the considered version
of QCB model appears to be soft